

Dalton Transactions

An international journal of inorganic chemistry

Accepted Manuscript

This article can be cited before page numbers have been issued, to do this please use: L. Ibáñez-Ibáñez, M. del Pico-Carranza, G. Guisado-Barrios and J. A. Mata, *Dalton Trans.*, 2026, DOI: 10.1039/D6DT00956E.



This is an Accepted Manuscript, which has been through the Royal Society of Chemistry peer review process and has been accepted for publication.

Accepted Manuscripts are published online shortly after acceptance, before technical editing, formatting and proof reading. Using this free service, authors can make their results available to the community, in citable form, before we publish the edited article. We will replace this Accepted Manuscript with the edited and formatted Advance Article as soon as it is available.

You can find more information about Accepted Manuscripts in the [Information for Authors](#).

Please note that technical editing may introduce minor changes to the text and/or graphics, which may alter content. The journal's standard [Terms & Conditions](#) and the [Ethical guidelines](#) still apply. In no event shall the Royal Society of Chemistry be held responsible for any errors or omissions in this Accepted Manuscript or any consequences arising from the use of any information it contains.

Visible-Light Assisted Dehydrogenation of Benzylamines Catalysed by a Standalone Ruthenium Complex.

Laura Ibáñez-Ibáñez,^a Mario del Pico-Carranza,^b Gregorio Guisado-Barrios^{*b} and José A. Mata^{*a}

Received 00th January 20xx,
Accepted 00th January 20xx

DOI: 10.1039/x0xx00000x

The dehydrogenation of benzyl amines to produce the corresponding nitriles and H₂ is an appealing strategy due to their application in hydrogen storage technologies. On the other hand, a wide range of current synthetic strategies to produce nitriles require a stepwise synthesis and severe reaction conditions. Here, we report an efficient visible-light promoted ruthenium(II) catalyzed hydrogen production from benzylic amines to the corresponding nitrile derivatives at room temperature and without additives. Our photocatalytic system comprises a single anionic 2-pyridonate based piano stool ruthenium precatalyst playing a dual role, harvesting visible-light and enabling H₂ generation in methanol. Mechanistic studies support pre-dissociation of the *p*-cymene ligand after light irradiation and formation of a solvato derivative that further enhances the catalytic activity towards nitrile formation.

Introduction

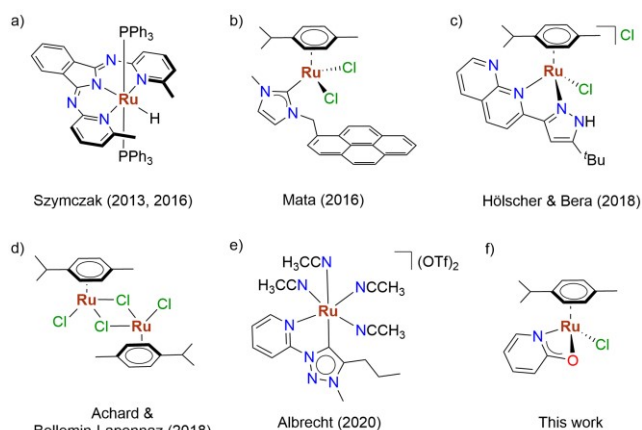
Acceptorless dehydrogenation (AD) of primary amines to nitriles, generating hydrogen as the only by-product has emerged as a valuable synthetic strategy due to its relevance to *Liquid Organic Hydrogen Carrier* (LOHC) technologies.^{1–3} LOHC systems rely on reversible transformations between H₂-lean and H₂-rich organic molecules, enabling safer and more sustainable hydrogen storage through sequential hydrogenation and dehydrogenation cycles.^{4–8} Furthermore, nitrile-containing compounds are key intermediates in pharmaceuticals, natural products, and industrial processes.^{9–11}

Traditional nitrile synthesis often requires toxic reagents, harsh conditions, and additives, leading to limited selectivity and significant environmental impact.¹² Consequently, the development of additive-free, efficient and sustainable dehydrogenation protocols has become a critical goal. Related amine-to-nitrile transformations have also been achieved via transfer or oxidative dehydrogenation using Ru and Ir complexes, in which hydrogen is either transferred to a sacrificial acceptor or consumed by an external oxidant rather than released as molecular hydrogen (H₂).^{13–16} For example, Brookhart and co-workers reported and Ir-catalysed system for the conversion of primary amines to nitriles using *tert*-butylethylene as hydrogen acceptor.¹⁶

Despite the advances, only a few highly selective AD systems for primary amines without external oxidants have been reported. Pioneering work by Szymczak and co-workers demonstrated the use of Ru(II)-H catalysts bearing a bis(2-pyridylimino)isoidolate ligand (Fig. 1a).^{17,18} Subsequently, we reported a N-heterocyclic carbene Ru(II)-NHC complex of formula [Ru^{II}(η^6 -*p*-cymene)(NHC)Cl₂], which showed moderate selectivity. However, incorporation of a pyrene moiety into the

NHC ligand, enabled immobilization on reduced graphene oxide (rGO), enhancing recyclability and showcasing its potential for H₂ storage.¹⁹ Likewise, a highly selective Ru(II) complex with a naphthyridine-functionalized pyrazole ligand was reported by Hölscher and Bera,²⁰ though required a strong base for optimal performance. Remarkably, Achard, Bellemin-Laponnaz and co-workers demonstrated that a simply [Ru^{II}(*p*-cymene)Cl₂]₂ alone could catalyse this transformation under oxidant and base-free conditions, with the amine substrate acting as ligand.²¹ More recently, Albrecht reported Ru(II)-mesoionic carbene (MIC) complexes [Ru^{II}(η^6 -*p*-cymene)(MIC)Cl₂] for aerobic amine dehydrogenation. In this system, *p*-cymene ligand dissociation in acetonitrile formed a solvato complex, enhancing activity and achieving up to 10.000 turnovers and 400 h⁻¹ TOF. However, water (not hydrogen) was produced as side-product.²²

More recently, acceptorless and oxidant-free dehydrogenation of amines to nitriles with H₂ evolution has also been reported using Ru-based systems, although these typically require elevated temperatures and/or additives.²³ Overall, these acceptorless systems remain predominantly thermally driven and typically require elevated temperatures or additives to overcome the intrinsic energetic barriers of dehydrogenation.²⁴



^a Institute of Advanced Materials (INAM), Universitat Jaume I, Avda. Vicent Sos Baynat s/n, 12006, Castellón (Spain).

^b Instituto de Síntesis Química y Catálisis Homogénea (ISQCH), CSIC-Universidad de Zaragoza, 50009, Zaragoza (Spain).

† Supplementary Information (ESI) available: See DOI: 10.1039/x0xx00000x



ARTICLE

Journal Name

Fig. 1. Examples of effective catalysts used in thermal dehydrogenation of primary amines to nitriles: a-d) Acceptorless dehydrogenation; e) Oxidative dehydrogenation; f) This work.

To overcome these limitations, attempts to use first-row transition metals such as Fe²⁵ or Co²⁶ have been explored, but these systems often suffer from low efficiency or still require strong bases and elevated temperatures.

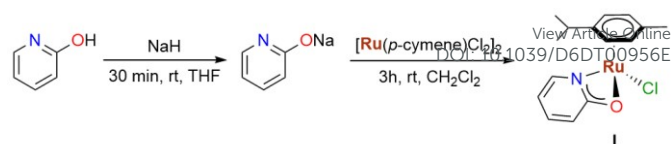
Alternatively, electrochemical,²⁷ and photocatalytic^{28,29} approaches have been investigated. Visible light, providing photon energies of 71-38 kcal/mol, can overcome activation barriers in many thermally driven reactions³⁰ and offers advantages in terms energy efficiency, waste minimization, and operational mildness. Photocatalytic oxidation of amines to nitriles using O₂ has been achieved with heterogeneous systems (e.g., Ru/TiO₂,³¹ Ru/γ-Al₂O₃²⁹) or homogenous systems combining [Ru^{II}(bpy)](Cl)₂ and a copper catalyst.³² However, these methods consume O₂, precluding hydrogen production. In parallel, photocatalytic dehydrogenative coupling (PDC) of amines to imines with hydrogen evolution has been achieved using (Pt@g-C₃N₄)²⁸ or CoP@ZnIn₂S₄ nanorods.³³ Yet, the partial dehydrogenation of amines to imines limits the amount of hydrogen yield compared to full conversion to nitriles.

A promising avenue involves the use of single metal complexes capable of both absorbing visible light and enabling catalytic bond transformation.^{30,34,35} For example, Miller *et al.* reported a [Cp*Ir(bpy-OMe)(Cl)]⁺ for photodehydrogenation of formic acid.³⁶ We previously demonstrated acceptorless dehydrogenation of N-heterocycles using a Ir(III)-MIC complex [Cp*Ir(MIC)(CH₃CN)]OTf under light irradiation.³⁷ Koenigs *et al.*, applied photoinduced Ru-catalysed C-C cross bond formation with [Ru^{II}(*p*-cymene)Cl₂]₂ and phosphoric acid diester.³⁸ Similarly, Ackermann and co-workers reported the Ru-catalysed visible-light hydroarylation³⁹ and ortho-C-H alkylation without external photosensitizers.⁴⁰

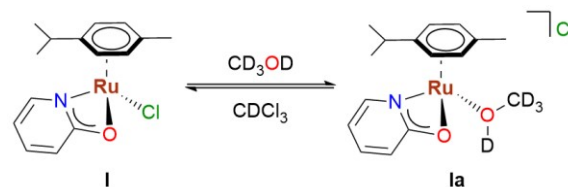
Building on these precedents, we recently reported H₂ generation via Ru(II)-catalysed photodehydrogenation of benzylic alcohols to carboxylates using a standalone NHC-Ru(II) complex of formula [RuCl₂(NHC)(η⁶-*p*-cymene)] featuring a NHC ligand having a methyl and pyrenylmethylene wingtips.⁴¹ Motivated by the need for efficient photocatalytic systems for hydrogen storage in LOHCs, we now describe the base- and oxidant-free photodehydrogenation of primary amines to nitriles under visible light irradiation at room temperature in methanol, catalysed by a single Ru(II) complex bearing a 2-pyridonate ligand (Fig. 1f).

Results and discussion

We commenced our study by preparing a ruthenium complex with a 2-pyridonate ligand by modifying a reported



Scheme 1. Synthesis of Ru(II) complex I.



Scheme 2. Equilibrium between Ru(II) complexes I and Ia in CD₃OD.

method.⁴² The neutral complex I of formula [Ru^{II}(η⁶-*p*-cymene)(κ²-O,N-(Opy)Cl)] was obtained in a two-step synthesis as an orange solid in a 92 % yield. Initially, 2-Hydroxypyridine was deprotonated with sodium hydride in tetrahydrofuran at room temperature for 30 minutes to form the corresponding alkoxide, which was further reacted with [Ru^{II}(*p*-cymene)Cl₂]₂ to

afford the desired compound (Scheme 1). Complex I was characterised by ¹H NMR and HR-MS (Fig. S1-S7).

The spectrum of I in CDCl₃ exhibits in the aliphatic region a singlet at 2.35 ppm corresponding to the methyl group along with a septuplet and a multiplet at 2.94 and 1.33 ppm respectively, that corresponds to the CH and the methyl groups of the isopropyl substituents of *p*-cymene ligand, whereas its aromatic protons can be observed in two sets at 5.62 and 5.37 ppm. In addition, the 2-pyridonate ligand exhibits four signals, two doublets at 7.84 and 6.05 ppm along with two triplets at 7.31 and 6.42 ppm. However, while this pattern is maintained in CD₃CN, a different behaviour was seen in CD₃OD, where the coexistence of two different species is observed. This speciation could be due to cleavage of the Ru-Cl bond prompted by the incorporation of a molecule of deuterated methanol into the coordination sphere of the metal centre forming complex Ia (Scheme 2). Interestingly, complex I can be recovered after removal of the solvent under vacuum, which has been confirmed after recording the ¹H NMR of the residue in CDCl₃ (Fig. S4).

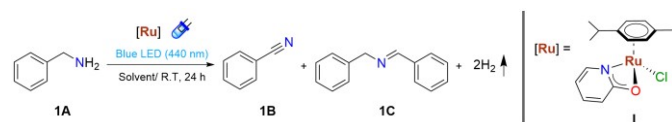
Catalytic properties

First, we explored the acceptorless photodehydrogenation of benzylamine **1A** as model reaction to produce the related benzonitrile **1B** and imine **1C** derivatives. The optimal reaction conditions (Table 1, entry 1) required 3 mol% of I, methanol as solvent, 24 hours irradiation and blue LEDs (440 nm) as light source under N₂ atmosphere but an open system (See photoreactor system ESI Fig. S40). Control experiments were conducted to ensure that the reaction does not proceed in the absence of catalyst or light (Table 1, entry 2-3). Diminishing the amount of catalyst resulted detrimental for the reaction (Entry 4). We observed that the selectivity of the dehydrogenation



reaction was largely dependent on the solvent used (Table 1, entries 5-11). Attempts to use less polar solvents, such as toluene, THF or *o*-dichlorobenzene provided lower conversions and selectivity towards the nitrile. In the case of CH₃CN (table 1, entry 8), a discrete ~25% conversion was obtained. Alcohol linear type solvents, such as MeOH or EtOH, provided the best catalytic outcome (Table 1, entry 1 and 10), so in this reaction it seems plausible that a polar coordinating solvent is needed for

Table 1. Optimization of the conditions.^[a]



Entry	Cat I (mol%)	Solvent (mL)	Light (nm)	Conv.	Select.	Select.
				(%) ^b A	(%) ^b B	(%) ^b C
1 ^a	3	CH ₃ OH	440	99	76	22
2	-	CH ₃ OH	440	9	0	99
3 ^c	3	CH ₃ OH	-	12	75	25
4	2	CH ₃ OH	440	69	65	26
5	3	THF	440	60	68	29
6	3	Tol	440	65	53	43
7	3	<i>o</i> -DCB	440	73	54	45
8	3	CH ₃ CN	440	25	51	49
9	3	CH ₂ Cl ₂	440	91	39	61
10	3	EtOH	440	99	77	22
11	3	ⁱ PrOH	440	99	55	42
12	3	CH ₃ OH	440 (25% int)	60	75	24
13	3	CH ₃ OH	525	53	74	23
14 ^d	3	CH ₃ OH	440	19	31	69
15 ^e	3	CH ₃ OH	440	99	75	23

^[a] Optimal Reaction conditions: 0.3 mmol of benzyl amine, catalyst I (3 mol%), room temperature, t = 24h, MeOH (1 mL), inert atmosphere, open system (bubbler), 45 W Kessil PR160L blue LEDs (440 nm, 100 % intensity). ^[b] Conversion and selectivity were determined by GC-FID using TMB (1,3,5-trimethoxybenzene) as internal standard. ^[c] At 50°C. ^[d] Inert atmosphere, closed system. ^[e] Air atmosphere, open system.

the reaction to proceed smoothly. Decreasing light intensity to 25% of the initially used (~39 mW/cm²) resulted in lower

conversions in 24h, thus, the use of 440 nm LED lamps at 100% intensity (~172 mW/cm²) was maintained. When using a less energetic LED lamp of 550 nm, a decrease in the conversion and selectivity was observed (Table 1, entry 13). To rule out the oxidation of amine rather than the dehydrogenation pathway, we performed an experiment under a closed system instead of

using a bubbler (table 1, entry 14). In this case, we have seen that closing the system resulted detrimental for the reaction, due to the impossibility of hydrogen to be released from the reaction media, which slows down the reaction. Interestingly, performing the reaction under air atmosphere in an open system (table 1, entry 15) provided similar conversion and selectivity than doing it under nitrogen atmosphere, which suggests that this reaction could be also performed by an oxidative pathway.

After having established the optimal reaction conditions for the photodehydrogenation of benzylamine, we wanted to explore the ligand and structure influence of ruthenium complexes in the catalytic outcome of the reaction (Fig. 2). For this purpose, we synthesized different ruthenium complexes bearing either chelating N-O (complexes I-III),⁴²⁻⁴⁴ N-N (complex IV),⁴⁵ C-N (complexes V-VI, for preparation see ESI) or monodentate carbon-based ligand (complex VII) ligands,⁴⁶ whose performance was evaluated in the visible light assisted dehydrogenation of benzylamines to nitriles with the concomitant formation of two molecules of H₂ (Fig. S8-S28).

Within this set, complex I of formula [Ru^{II}(η⁶-*p*-cymene)(κ²-N,O-(Opy)Cl)] bearing the 2-pyridonate ligand resulted in the most efficient catalyst, reaching full conversion of **1A** and yielding the benzonitrile **1B** and *N*-benzylbenzaldimine **1C** products in a 76 % and 22% respectively. The related quinolin-2-olate derived complex II featuring an additional benzene ring in the 2-pyridonate motif, exhibited similar activity.

In contrast, the quinolin-8-olate based analogue III resulted far less efficient. Complex IV containing N,N chelating 6,6'-dihydroxy-2,2'-bipyridine ligand displayed moderate conversion



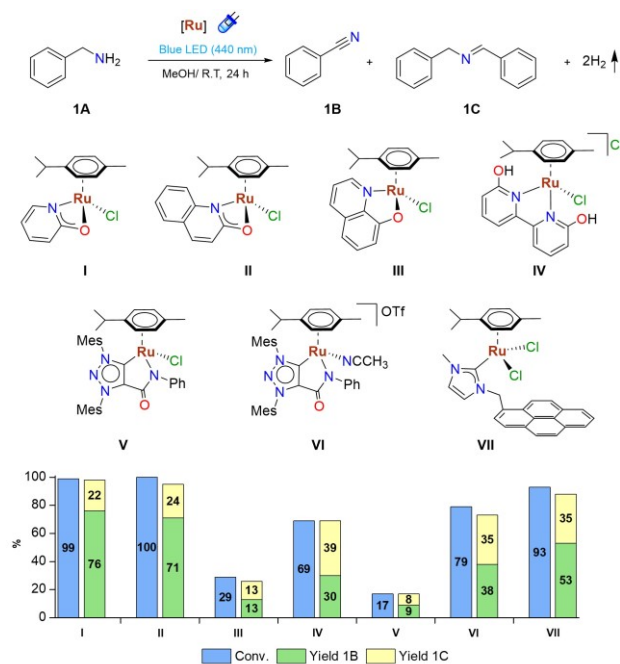


Fig. 2. Schematic representation of Ru(II) complexes I-VII used in this study. Reaction conditions: 0.3 mmol of benzylamine **1A**, ruthenium complexes I-VII (3.0 mol%), MeOH (1 mL), room temperature, $t = 24$ h, $\lambda = 440$ nm, inert atmosphere and open system (bubbler). Conversions and yields obtained by GC-FID using 1,3,5-trimethoxybenzene as internal standard.

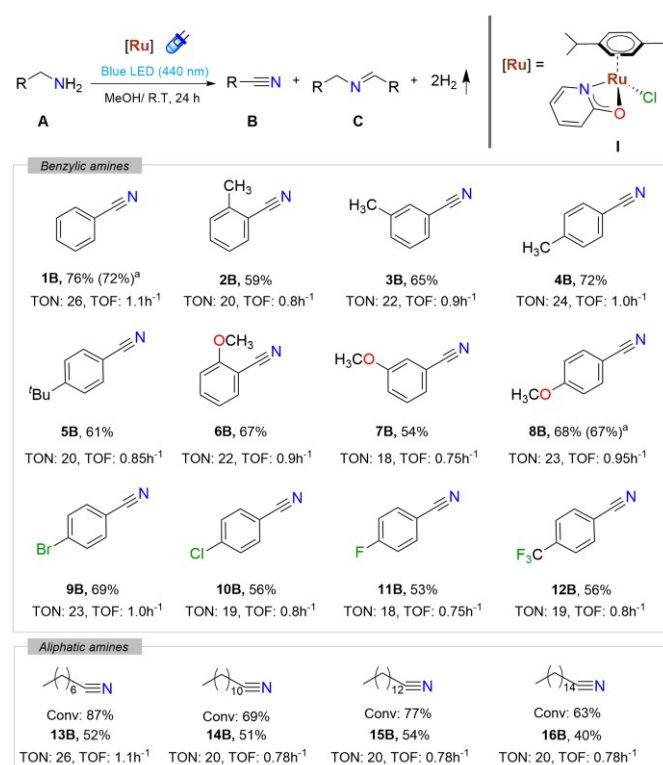


Fig. 3. Photocatalytic dehydrogenation of benzylic amines derivatives **1-12B** and aliphatic amines **13-16B**. Reaction conditions: 0.3 mmol of substrate, $t = 24$ h, blue LED $\lambda = 440$ nm, MeOH (1 mL), 3.0 mol% **I**, room temperature, inert atmosphere (N₂), open system (bubbler).

Yields determined by GC-FID using 1,3,5-trimethoxybenzene as internal standard. ^aIsolated yields. DOI: 10.1039/D6DT00956E

and inferior selectivity towards the nitrile product. Among the neutral **V** and cationic **VI** complexes bearing a mesoionic triazolylidene (MIC) ligand with an amido functionality, only **VI** exhibited good conversion but low selectivity. This result contrast with the good catalytic performance obtained when



using the Ir(MIC) analogues in the light-promoted dehydrogenation of N-heterocycles.³⁷

Finally, complex **VII** having an NHC ligand with a pyrene tag, albeit displaying high conversion resulted less selective than complex **I**. Thus, the presence of the 2-pyridonate ligand was found necessary to reach the highest activity and selectivity.

It is worth mentioning that related complexes that possess this ligand have shown good activity towards hydrofunctionalization reactions, such as the dehydrogenation of alcohols.⁴⁷⁻⁴⁹

To gain a better insight about the observed photocatalytic performance of complexes **I-VII** their UV-Vis absorption spectra were recorded in methanol (Fig. S29).

However, no significant differences among them with respect to complex **I** were observed, preventing a direct correlation between absorption properties and catalytic outcome.

Additionally, the absorption and excitation spectra of complex **I** were recorded (Fig. S30), allowing estimation of the 0-0 transition energy (E_{0-0}) with a value of 3.6 eV. Cyclic voltammetry measurements were also performed to evaluate

its redox properties exhibiting an irreversible oxidation event at 0.78 V and an irreversible event at -1.91 V vs Fc/Fc⁺.

Based on these values, the excited state redox potentials were estimated with the Rehm-Weller's equation, giving approximate values of $E^*_{red} = 1.691$ V and $E^*_{ox} = -2.823$ V vs Fc/Fc⁺ (Fig. S31-33). These values provide inside into the electronic properties of the photoexcited species, although no direct redox pathway is proposed in the present catalytic mechanism.

After evaluating the catalytic performance of all ruthenium complexes, we inspected the scope of several benzyl and alkyl amines under the optimal reaction conditions using catalyst **I**.

The outcomes of these catalytic studies are included in (Fig. 3). It can be drawn that conversion was quantitative after 24h for all the substrates. Of them, benzonitrile **1C** was produced in a 76 % yield. In parallel, the related substituted benzonitriles bearing electron donating alkyl group (**2B-5B**) were obtained high yields. In contrast, those analogues having electron withdrawing chloride, fluoride or trifluoromethyl substituents

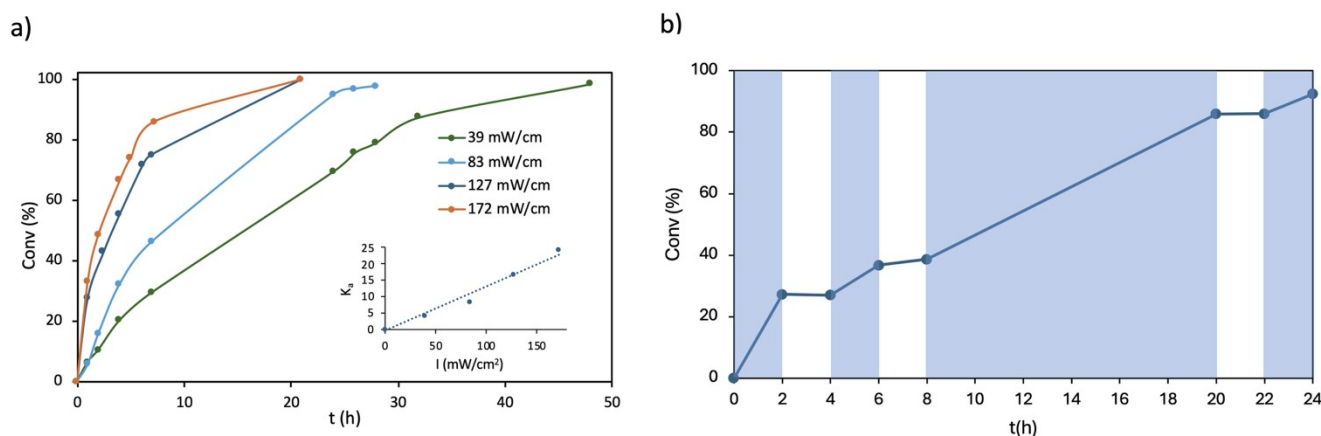


Fig. 4. a) Light intensity experiment. Reaction conditions: 0.3 mmol of benzylamine, catalyst **I** (3.0 mol%), MeOH (1 mL), room temperature, $\lambda = 440$ nm at different intensities, inert atmosphere and open system (bubbler). Inset: reaction rate constant (K_a) vs light intensity using the initial reaction rates. b) ON/OFF experiment. Reaction conditions: 0.3 mmol of benzylamine, catalyst **I** (3.0 mol%), MeOH (1 mL), room temperature, $\lambda = 440$ nm irradiation at selected times (in blue), inert atmosphere and open system



ARTICLE

View Article Online
DOI: 10.1039/D6DT00956E

in 59 – 72% yield. Similarly, benzonitriles containing electron donating methoxy group (**6B- 8B**) were obtained in relatively (**10B- 12B**) were obtained in moderate yields (56%). Bromide substitution (**9B**) gave higher yield (69%). Aliphatic amines were also evaluated under the standard reaction conditions (Fig. 3, **13B-16B**). In these cases, lower conversions were observed compared to benzylic amines after 24 h, although selectivity towards the corresponding nitriles maintained comparable.

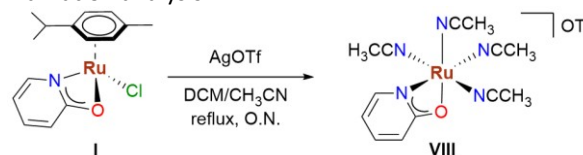
Mechanistic Studies

After evaluating the scope of substrates, we performed a set of experiments to gain some insight into the reaction mechanism. First, the formation of hydrogen as by-product in the reaction was confirmed qualitatively by GC-TCD chromatography (Fig. S45-S46). To detect hydrogen, reaction was scaled up (1.5 mmol of substrate) and was performed in a closed system to accumulate hydrogen. As previously seen in Table 1, entry 14, photodehydrogenation was slowed down when the system is closed, as hydrogen cannot be released from the reaction media. The headspace of the reaction was analysed by GC-TCD, confirming the presence of H₂, which demonstrates that it is a dehydrogenation process rather than an oxidative pathway.

Then, we wanted to explore the influence of blue light in the reaction. Thus, we performed an experiment evaluating the light intensity effect in the photodehydrogenation using catalyst **I** (Fig. 4a). A linear dependence of light intensity vs activity was found, as we have previously observed in other photocatalytic reaction (Fig. 4a, inset).⁵⁰ Since saturation was negligible, the highest intensity (172 mW/cm²) was maintained to obtain the best catalytic outcome. The role of light was also assessed by an on/off experiment (Fig. 4b). In this case, we monitored the conversion in the dehydrogenation of benzylamine with and without light irradiation at selected times until completion. We disclosed that reaction conversion increased when lights were switched on, but it remained almost unchanged when light was off. These results confirmed that blue light is essential for the reaction to proceed, and it is needed throughout all reaction and not only to obtain active catalytic species.

Once the influence of light in the reaction was evaluated, we monitored the course of the reaction at different catalyst loadings (Fig. S47-S48). In this case, we observed that complete conversion was achieved after 24h using 3.0 mol% of catalyst **I**. Interestingly, selectivity ratio was maintained throughout the reaction (~75/25% of nitrile/imine). Variation of catalyst loading from 3.0 to 0.75 mol% showed a clear decrease in activity, yet the photodehydrogenation of amines still proceeds at lower catalyst loadings (78% conversion after 48h at 0.75 mol% catalyst loading). We calculated the order in

catalyst using the graphical method of variable time normalization analysis



Scheme 3. Synthesis of solvato complex **VIII**.

(VTNA).^{51,52} The results suggest that the photodehydrogenation of amines using complex **I** is first-order dependent on catalyst concentration, indicating that reaction rate is linearly proportional to the amount of complex (Fig. S49).

Next, reaction monitoring by ¹H NMR spectroscopy was performed. To do that, we used *p*-methoxybenzylamine under optimal reaction conditions using deuterated methanol to record ¹H NMR spectra at selected times, which showed the disappearance of benzylamine signals and subsequent formation of nitrile and imine products (Fig. S50). Interestingly, two extra new weak signals at 2.27 ppm (singlet) and 1.20 ppm (doublet) were observed after 2h of irradiation. To confirm whether these new signals correspond to the presence of a third product or catalyst derivatization, two additional monitoring experiments were performed. Firstly, we performed a pseudophotocatalytic experiment using a high catalyst loading for ¹H NMR monitoring (Fig. S51). During the reaction, we could see the disappearance of the initial catalyst's signals. Formation of new signals that can be attributed to free *p*-cymene ligand were observed, which indicates that decoordination has taken place (Fig. S52). This process has been previously described by Albrecht in the dehydrogenation of amines using a Ru(II)-MIC complex.²² In their case, they

reported complete *p*-cymene dissociation after thermally induced activation, when conducting the reaction at 150 °C. More recently, Ackermann described *p*-cymene light-induced dissociation at room temperature in the blue-assisted hydroarylation of unactivated olefins using [Ru(OAc)₂(*p*-cymene)] precatalyst.³⁹ To certify if in our case its dissociation was light promoted, a solution of complex **I** was irradiated with blue light (Fig. S53). It was confirmed that the peaks (around 6.0- 5.0 ppm) corresponding to the coordinated *p*-cymene ligand completely vanish after 16h. As a result, it could be speculated the formation of a solvato complex where the ruthenium centre is coordinated to the pyridonate ligand along with four molecules of methanol completing the coordination sphere. In parallel, colour change from yellow to dark brown was noted while the catalytic reaction was performed (Fig. S54). Similar change was also witnessed when we irradiated complex **I**, suggesting that blue visible light induced the formation of new active species that lack the *p*-cymene moiety.



Next, we monitored the reaction by UV-Vis registering the spectrum at different reaction times (Fig. S55). The appearance of a new band in the blue region of the absorption spectrum could be seen after light irradiation, suggesting that new catalytically active species are formed. Visually, reaction

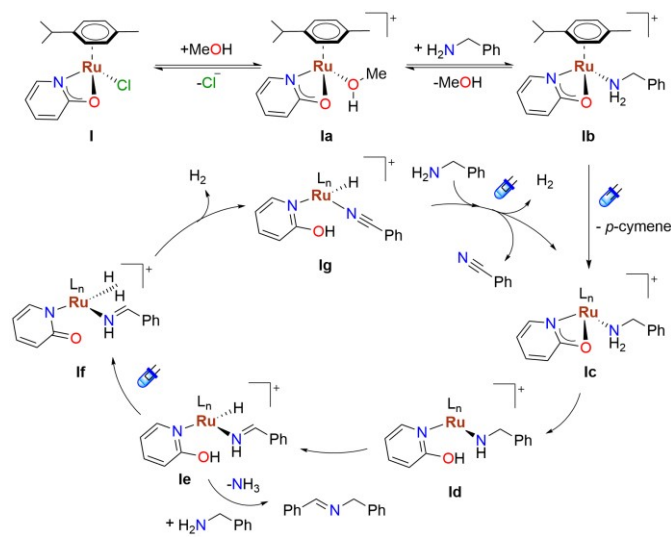


Fig. 5 Proposed catalytic cycle for the photodehydrogenation of benzylamines.

changes progressively from yellow, to reddish, brownish and finally dark brown. To discard that the observed colour change is due to the formation of heterogeneous Ru species, poisoning experiments using either Hg (mercury test) as NPs scavenger or P4VP (molecular species scavenger) were performed (Fig. S56), as well as a filtration experiment at an intermediate reaction time (Fig. S57). The results support the predominance of homogeneous Ru species in solution under the reaction conditions.

Then, to check if a solvato complex could be able to catalyse the reaction in a similar manner that catalyst **I**, we carried out the synthesis and isolation of a related solvato complex **VIII** of formula $[\text{Ru}^{\text{II}}(\text{CH}_3\text{CN})_4(\kappa^2\text{-N,O}(\text{Opy}))\text{OTf}]$ (Scheme 3). The new complex was prepared by reacting **I** with AgOTf in a mixture of dichloromethane/acetonitrile which was isolated as a brown solid in a 65% yield. The solvato complex was fully characterized by NMR spectroscopy, mass spectrometry and UV-Vis spectroscopy (Fig. S34-39). The photocatalytic properties of complex **VIII** were evaluated under the optimal reaction conditions and displayed similar activity to complex **I** (Table S1). This result may suggest that a related solvato complex of formula $[\text{Ru}^{\text{II}}(\text{CH}_3\text{OH})_4(\kappa^2\text{-N,O}(\text{Opy}))\text{Cl}]$ could be an intermediate in the reaction. Unfortunately, all our attempts to isolate a solvato complex containing four methanolic ligands failed.

Additional mechanistic studies were carried out to detect any possible intermediate in the reaction by ESI-MS spectrometry. Interestingly, we could see that before light irradiation, a new species containing a coordinated benzylamine (**Ib**) could be detected, which was presumably formed by the replacement of a MeOH molecule in **Ia**

(Fig. S58-S59). Then, an aliquot was analysed after 2 h of reaction, and the ESI-MS spectrum was recorded, however, the observed products could not be unambiguously assigned. Despite that, we could see mass fragmentations of a difference of $m/z=105$, which corresponds to the benzylimine product, which could mean that reaction is taking place through coordination of several benzylamines to the complex vacancies followed by dehydrogenation.

Based on the above experiments, we propose a plausible mechanism for the photodehydrogenation of benzylamines to benzonitriles (Fig. 5). The neutral complex **I** $[\text{Ru}^{\text{II}}(\eta^6\text{-p-cymene})(\kappa^2\text{-N,O}(\text{Opy}))\text{Cl}]$ is first solubilised in methanol to give the cationic species **Ia** following chloride substitution by solvent, as observed by ^1H NMR spectroscopy. In the presence of benzylamine, **Ia** is converted into **Ib** $[\text{Ru}^{\text{II}}(\eta^6\text{-p-cymene})(\kappa^2\text{-O,N}(\text{Opy})(\text{PhCH}_2\text{NH}_2))\text{Cl}]$, as indicated by ESI-MS analysis. Upon visible light irradiation, dissociation of the *p*-cymene ligand affords the solvato complex **Ic**. Subsequently, ligand assisted deprotonation of the coordinated amine is proposed to generate **Id**, which may undergo β -hydride elimination to form a putative Ru-H **Ie**. We were unable to directly detect this Ru-H species by NMR, likely due to its transient nature and high reactivity. However, a trapping experiment using tritylium tetrafluoroborate as a hydride scavenger resulted in a decrease in the reaction rate (Fig. S60), providing indirect evidence for the involvement of Ru-H intermediates. This proposal is consistent with established mechanistic proposals for acceptorless dehydrogenation reactions involving β -hydride elimination and metal-hydride intermediates.¹⁵ Indirect evidence for the formation of coordinated imine species was obtained by HR-MS experiments. The reaction with a second benzylamine is proposed to release the imine intermediate. Further protonation and β -hydride elimination steps may involve additional Ru-H species, ultimately resulting in the release of two equivalents of H_2 and formation of benzonitrile. Finally, coordination of a new benzylamine molecule regenerates the active catalysts, closing the catalytic cycle.

Experimental

The complete experimental section is included in the Supporting Information.

Conclusions

In summary, we report the photocatalytic ruthenium catalysed dehydrogenation of primary amines to the corresponding nitriles with concomitant H_2 evolution. The system operates under visible-light irradiation using a single 2-pyridonate-Ru^{II} complex, which acts as both light absorber and catalysts, enabling the transformation under mild conditions in methanol without the need for external oxidants or photosensitizers.

Mechanistic studies are consistent with photoinduced dissociation of the *p*-cymene ligand to form a more reactive solvato species, which is proposed to participate in the



ARTICLE

Journal Name

catalytic cycle leading to nitrile formation and H₂ release. Despite the moderate yields obtained, this work represents to best of our knowledge, one of the first examples of photo dehydrogenation of amines to nitriles with H₂ evolution under oxidant-free conditions. These findings highlight the potential of molecular Ru complexes as platforms for the development of light-driven acceptorless dehydrogenation processes relevant to hydrogen storage technologies.

Author contributions

Laura Ibañez-Ibañez and Mario del Pico-Carranza contributed to methodology, validation, investigation and formal analysis of results as well as writing-review and editing. Gregorio Guisado-Barrios and José A. Mata contributed to conceptualizing formal analysis, resources, writing original draft, writing-review and editing and funding acquisition.

Conflicts of interest

There are no conflicts to declare.

Data availability

Experimental details, synthetic procedures, spectroscopic data, and catalytic studies are included in the ESI.

Acknowledgements

J.A.M thanks to PID2021-126071OB-C22 and Thematic Network "OASIS" RED2022-134074-T financed by MICIN/AEI/10.13039/501100011033/FEDER "Una manera de hacer Europa", Generalitat Valenciana (MFA/2022/043) with funding from European Union NextGenerationEU and Universitat Jaume I (UJI-B2022-23). G.G.-B. gratefully acknowledges PID2021-122900NB-I00 funded by MICIN/AEI/10.13039/501100011033/FEDER "Una manera de hacer Europa" and MCIN/AEI/10.13039/501100011033 "Next Generation EU"/PRTR/CNS2023-143731, Gobierno de Aragón/FEDER, UE (DGA/FEDER, UE (GA/FEDER, Arquitectura Molecular Inorgánica y Aplicaciones, Group E50_23R) and 2024ICT332 funded by CSIC (Ayudas Incorporación Científicos Titulares OPIS). L.I.-I. thanks MICIU (FPU20/04385) for a predoctoral contract. The authors thank "Servei Central d'Instrumentació Científica (SCIC) de la Universitat Jaume I". The authors would like to acknowledge the use of "Servicio General de Apoyo a la Investigación-SAI, Universidad de Zaragoza".

References

1 P. K. R. Shaheen and A. Sarbajna, *Coord. Chem. Rev.*, 2026, **547**, 217095.

- 2 D. L. J. Broere, *Phys Sci Rev*, 2018, **3**, 20170029. View Article Online
DOI: 10.1039/D6DT00956E
- 3 R. H. Crabtree, *ACS Sustain. Chem. Eng.*, 2017, **5**, 4491–4498.
- 4 P. M. Modisha, C. N. M. Ouma, R. Garidzirai, P. Wasserscheid and D. Bessarabov, *Energy Fuels*, 2019, **33**, 2778–2796.
- 5 P. T. Aakko-Saksa, C. Cook, J. Kiviaho and T. Repo, *J. Power Sources*, 2018, **396**, 803–823.
- 6 P. Preuster, C. Papp and P. Wasserscheid, *Acc. Chem. Res.*, 2017, **50**, 74–85.
- 7 C. Chu, K. Wu, B. Luo, Q. Cao and H. Zhang, *Carbon Resour. Convers.*, 2023, **6**, 334–351.
- 8 V. Yadav, G. Sivakumar, V. Gupta and E. Balaraman, *ACS Catal.*, 2021, **11**, 14712–14726.
- 9 G. Yan, Y. Zhang and J. Wang, *Adv. Synth. Catal.*, 2017, **359**, 4068–4105.
- 10 F. F. Fleming, L. Yao, P. C. Ravikumar, L. Funk and B. C. Shook, *J. Med. Chem.*, 2010, **53**, 7902–7917.
- 11 F. F. Fleming, *Nat. Prod. Rep.*, 1999, **16**, 597–606.
- 12 R. K. Grasselli, *Catal. Today*, 1999, **49**, 141–153.
- 13 K. Müller, *Energy Technol.*, 2022, **10**, 202200468.
- 14 J. Choi, A. H. R. MacArthur, M. Brookhart and A. S. Goldman, *Chem. Rev.*, 2011, **111**, 1761–1779.
- 15 Caroline J. Verhoef, R. Ma and J. C. Sloopweg, *Chem. Rev.*, 2026, DOI:10.1021/acs.chemrev.5c00904.
- 16 W. H. Bernskoetter and M. Brookhart, *Organometallics*, 2008, **27**, 2036–2045.
- 17 K.-N. T. Tseng, A. M. Rizzi and N. K. Szymczak, *J. Am. Chem. Soc.*, 2013, **135**, 16352–16355.
- 18 L. V. A. Hale, T. Malakar, K.-N. T. Tseng, P. M. Zimmerman, A. Paul and N. K. Szymczak, *ACS Catal.*, 2016, **6**, 4799–4813.
- 19 D. Ventura-Espinosa, A. Marzá-Beltrán and J. A. Mata, *Chem. A Eur. J.*, 2016, **22**, 17758–17766.
- 20 I. Dutta, S. Yadav, A. Sarbajna, S. De, M. Hölscher, W. Leitner and J. K. Bera, *J. Am. Chem. Soc.*, 2018, **140**, 8662–8666.
- 21 T. Achard, J. Egly, M. Sigrist, A. Maise-François and S. Bellemin-Laponnaz, *Chem. A Eur. J.*, 2019, **25**, 13271–13274.
- 22 M. Olivares, P. Knörr and M. Albrecht, *Dalton Trans.*, 2020, **49**, 1981–1991.
- 23 S. Yadav and R. Gupta, *Dalton Trans.*, 2025, **54**, 5675–5684.



- 24 M.-J. Zhou, G. Liu, C. Xu and Z. Huang, *Synthesis*, 2022, **55**, 547–564.
- 25 A. S. Nanuwa, M. D. Hoffman, K. Nandi and J. M. Blacquièrre, *Organometallics*, 2024, **43**, 2342–2348.
- 26 H. Tian, C.-Y. Ding, R.-Z. Liao, M. Li and C. Tang, *J. Am. Chem. Soc.*, 2024, **146**, 11801–11810.
- 27 N. Guenani, J. Solera-Rojas, D. Carvajal, C. Mejuto, A. Mollar-Cuni, A. Guerrero, F. Fabregat-Santiago, J. A. Mata and E. Mas-Marzá, *Green Chem.*, 2024, **26**, 8768–8776.
- 28 P. Bai, G. Yang, H. Sun and X. Tong, *Green Chem. Eng.*, 2022, **3**, 313–320.
- 29 P. Zhu, J. Zhang, J. Wang, P. Kong, Y. Wang and Z. Zheng, *Catal. Sci. Technol.*, 2019, **10**, 440–449.
- 30 W.-M. Cheng and R. Shang, *Acs Catal.*, 2020, **10**, 9170–9196.
- 31 D. S. Ovoshchnikov, B. G. Donoeva and V. B. Golovko, *ACS Catal.*, 2015, **5**, 34–38.
- 32 C. Tao, B. Wang, L. Sun, Z. Liu, Y. Zhai, X. Zhang and J. Wang, *Org. Biomol. Chem.*, 2016, **15**, 328–332.
- 33 W. Liu, Y. Wang, H. Huang, J. Wang, G. He, J. Feng, T. Yu, Z. Li and Z. Zou, *J. Am. Chem. Soc.*, 2023, **145**, 7181–7189.
- 34 F. Juliá, *ACS Catal.*, 2025, 4665–4680.
- 35 K. P. S. Cheung, S. Sarkar and V. Gevorgyan, *Chem. Rev.*, 2022, **122**, 1543–1625.
- 36 S. M. Barrett, S. A. Slattery and A. J. M. Miller, *ACS Catal.*, 2015, **5**, 6320–6327.
- 37 C. Mejuto, L. Ibáñez-Ibáñez, G. Guisado-Barrios and J. A. Mata, *ACS Catal.*, 2022, **12**, 6238–6245.
- 38 S. Jana, C. Pei, S. B. Bahukhandi and R. M. Koenigs, *Chem Catal.*, 2021, **1**, 467–479.
- 39 S. Trienes, S. Golling, M. H. Gieuw, M. D. Matteo and L. Ackermann, *Chem. Sci.*, 2024, **15**, 19037–19043.
- 40 Y. Wang, B. Yuan, X. Chang and L. Ackermann, *Chem*, 2025, **11**, 102387.
- 41 L. Ibáñez-Ibáñez, G. Guisado-Barrios and J. A. Mata, *J. Catal.*, 2025, **448**, 116134.
- 42 P. Lahuerta, J. Latorre, M. Sanaú, F. A. Cotton and W. Schwotzer, *Polyhedron*, 1988, **7**, 1311–1316.
- 43 Z. Sahli, B. Sundararaju, M. Achard and C. Bruneau, *Green Chem.*, 2013, **15**, 775–779.
- 44 S. L. Nongbri, B. Therrien and K. M. Rao, *Inorg. Chim. Acta*, 2011, **376**, 428–436. View Article Online
DOI: 10.1039/D6DT00956E
- 45 I. Nieto, M. S. Livings, J. B. Sacci, L. E. Reuther, M. Zeller and E. T. Papish, *Organometallics*, 2011, **30**, 6339–6342.
- 46 S. Sabater, J. A. Mata and E. Peris, *ACS Catal.*, 2014, **4**, 2038–2047.
- 47 K. Fujita, N. Tanino and R. Yamaguchi, *Org. Lett.*, 2007, **9**, 109–111.
- 48 A. M. Royer, T. B. Rauchfuss and D. L. Gray, *Organometallics*, 2010, **29**, 6763–6768.
- 49 A. Fedulin and A. J. von Wangelin, *Catal. Sci. Technol.*, 2023, **14**, 26–42.
- 50 L. Ibáñez-Ibáñez, A. Lázaro, C. Mejuto, M. Crespo, C. Vicent, L. Rodríguez and J. A. Mata, *J. Catal.*, 2023, **428**, 115155.
- 51 C. D.-T. Nielsen and J. Burés, *Chem. Sci.*, 2018, **10**, 348–353.
- 52 J. Burés, *Angew. Chem.*, 2016, **128**, 2068–2071.



Data Availability Statement

The data supporting the findings of this study are included in the Supplementary Information (ESI).

